

Anomalous electrical performance of nanoscaled interfacial oxides for bonded n - GaAs wafers

Hao Ouyang, YewChung Sermon Wu, Hsiao-Hao Chiou, Chia-Cheng Liu, Ji-Hao Cheng, Wen Ouyang, Shan-Haw Chiou, Sham-Tsong Shiue, Y. L. Chueh, and L. J. Chou

Citation: *Applied Physics Letters* **88**, 112112 (2006); doi: 10.1063/1.2185611

View online: <http://dx.doi.org/10.1063/1.2185611>

View Table of Contents: <http://scitation.aip.org/content/aip/journal/apl/88/11?ver=pdfcov>

Published by the [AIP Publishing](#)

Articles you may be interested in

Effect of interfacial reactions between atomic-layer-deposited HfO₂ films and n -GaAs (100) substrate using postnitridation with NH₃ vapor

Appl. Phys. Lett. **97**, 092113 (2010); 10.1063/1.3481801

Local etching of nanoholes and quantum rings with In_xGa_{1-x} droplets

J. Appl. Phys. **106**, 064315 (2009); 10.1063/1.3225759

First-principles analysis of interfacial nanoscaled oxide layers of bonded N - and P -type GaAs wafers

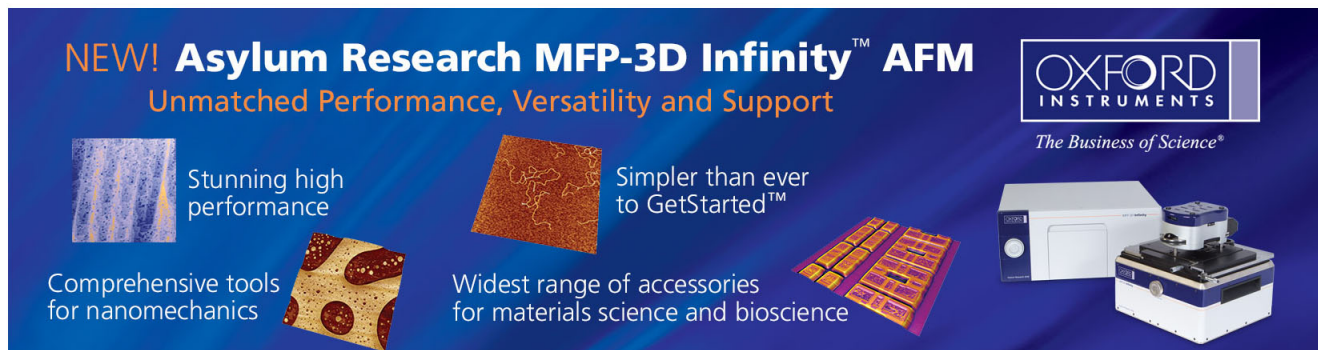
J. Appl. Phys. **102**, 013710 (2007); 10.1063/1.2748335

Current-voltage characteristics of p - GaAs / n - GaN heterojunction fabricated by wafer bonding

Appl. Phys. Lett. **90**, 102107 (2007); 10.1063/1.2710750

Nanoscaled interfacial oxide layers of bonded n - and p -type GaAs wafers

Appl. Phys. Lett. **88**, 172104 (2006); 10.1063/1.2198511



NEW! Asylum Research MFP-3D Infinity™ AFM
Unmatched Performance, Versatility and Support

OXFORD INSTRUMENTS
The Business of Science®

Stunning high performance

Simpler than ever to GetStarted™

Comprehensive tools for nanomechanics

Widest range of accessories for materials science and bioscience

Asylum Research

Anomalous electrical performance of nanoscaled interfacial oxides for bonded *n*-GaAs wafers

Hao Ouyang^{a)}

Department of Materials Engineering, National Chung Hsing University, Taichung 402, Taiwan, Republic of China

YewChung Sermon Wu

Department of Materials Science and Engineering, National Chiao Tung University, Hsinchu 300, Taiwan, Republic of China

Hsiao-Hao Chiou and Chia-Cheng Liu

Department of Materials Engineering, National Chung Hsing University, Taichung 402, Taiwan, Republic of China

Ji-Hao Cheng

Department of Materials Science and Engineering, National Chiao Tung University, Hsinchu 300, Taiwan, Republic of China

Wen Ouyang

Chung-Hua University, Department of Computer Science and Information Engineering, 707, Sec.2, WuFu Rd., Hsinchu, Taiwan 300, Republic of China

Shan-Haw Chiou

Materials Research Laboratories, Industrial Technology Research Institute, Hsinchu 300, Taiwan, Republic of China

Sham-Tsong Shiue

Department of Materials Engineering, National Chung Hsing University, Taichung 402, Taiwan, Republic of China

Y. L. Chueh and L. J. Chou

Department of Materials Science and Engineering, National Tsing Hua University, Hsinchu 300, Taiwan, Republic of China

(Received 7 November 2005; accepted 17 February 2006; published online 16 March 2006)

Electrical performance was found to be closely related to the variation of nanosized interface morphology in previous studies. This work investigated in detail the microstructural development of in- and anti-phase bonded interfaces for *n*-type (100) GaAs wafers treated at 500, 600, 700 and 850 °C. The interfacial energy of anti-phase bonding is higher than that of in-phase bonding based on the first-principles calculations. The higher interface energy tends to stabilize the interfacial oxide layer. The continuous interfacial oxide layer observed below 700 °C can deteriorate the electrical property due to its insulating property. However, the existence of nanoscaled oxide at anti-phase bonded interfaces can improve the electrical conductivity at 700 °C. This is due to the suppression of the evaporation of As atom by the interfacial nanoscaled oxides based on the analysis of autocorrelation function and energy dispersive x-ray spectroscopy. © 2006 American Institute of Physics. [DOI: 10.1063/1.2185611]

Conventional heteroepitaxial growth techniques applied to lattice mismatched active layers usually result in a high density of threading dislocations in the bulk of samples. Direct bonding of single crystalline wafers of similar or dissimilar materials is a unique alternative approach to the epitaxial growth.¹ Bonding of III-V semiconductors was originally developed for two-layer optoelectronic devices.²⁻⁴ Bonding was usually performed at elevated temperatures to raise the bonding strength and bonded area.^{5,6} Recently, direct wafer bonding has enabled the development of many state-of-the-art photonic devices.⁷ For many optoelectronic device applications, the active layers are essential to have high crystallographic quality with interfaces that are thermally and electrically conductive, and almost optical loss

free.¹ It was found that *n*-type GaAs did not bond directly to itself, but instead via a nanosized amorphous oxide layer at 500 °C in former work.⁸ Similar condition was observed for the *p*-type GaAs but at lower temperature.⁹ In this study, the influence of bonding phase on the electrical performance after thermal annealing was investigated.

This study used Si-doped ($4 \times 10^{18}/\text{cm}^3$) *n*-type (100) GaAs wafers. The detailed procedures can be found in a previous investigation.⁸ Two groups of wafers clarified by in- and anti-phase bondings were prepared to examine the effects of crystallographic orientation on the morphological evolution and electrical performance. In the first group, which corresponds to anti-phase direct bonding, the [110] axes of the two wafers were aligned to be parallel, making the lattice structure symmetric at the bonding interface. This structure is unusual since it cannot be obtained by epitaxial growth.¹⁰ The other group was prepared with in-phase direct

^{a)} Author to whom correspondence should be addressed; electronic mail: houyang@nchu.edu.tw

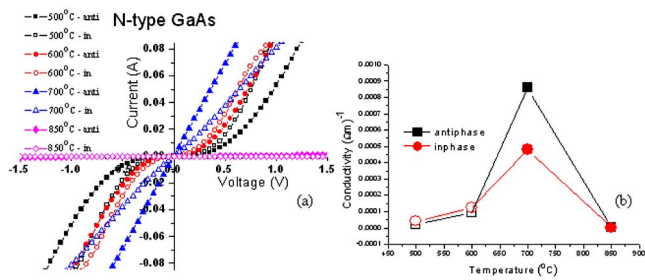


FIG. 1. (Color online) (a) Current-voltage characteristic of in-phase and anti-phase bonded two-layer *n*-type (100) GaAs wafers processed at fixed temperatures varied from 500 to 850 °C for 2 h in argon ambient. (b) Corresponding conductivity calculated from (a), the open symbols are from nonlinear curves.

bonding, in which the lattice order retains the same zinc blende structure throughout both bonded wafers, making the [110] axis of the GaAs wafer perpendicular to the [110] axis of the other wafer. Argon-ambient annealings were taken basically at 400, 500, 600, 700 and 850 °C. Single GaAs wafers were processed under identical thermal conditions and were utilized to separate the bulk and surface effects from the interfacial effects.⁸ For this study, bonded wafers were then diced into 2×2 mm². Only samples from the central portions of the bonded wafers were investigated.

It was discovered that there exists a continuous interfacial oxide in the bonded wafers treated at lower temperature (below 700 °C).^{8,9} This oxide layer has been identified as mainly the amorphous Ga₂O₃ and was found to behave as an insulating layer by first-principle calculations and experimental measurements in our former work.⁹ Therefore, the nonlinear behavior of current versus voltage observed is related to the potential barrier formed at the continuous oxide interface as shown in Fig. 1(a). Using Ohm's law and the conductivity σ as presented in Fig. 1(b) can be obtained from

$$\sigma = L/RA, \quad (1)$$

where L , A are the thickness and area of sample, respectively, and R is the resistance.¹¹ For the nonlinear I - V curve, the conductivity was calculated by arbitrarily choosing the value at 0.2 V and was indicated by the open symbol in Fig. 1(b). Other choices like 0.5 V give similar results and the data at 700 °C discussed most often later is from linear parts in Fig. 1(a). The conductivity improves as the treated temperature increases from 500 to 700 °C due to the expansion of bonded area between the samples.^{8,9} The nonlinear or linear curves for both in-phase and anti-phase bonded samples treated at the same temperature do not show a large current difference as that at 700 °C at a fixed voltage. It is more obvious to see this with the illustration in Fig. 1(b). The result for the sample treated at 850 °C will be explained later.

It was found that more oxide tends to stay in the interface for the anti-phase bonding probably due to the higher interfacial energy of the anti-phase interface at 600 °C.⁹ In order to confirm this surmise, we conducted a first-principles calculation using the density function approximation. The total free energy per cell was obtained according to the generalized gradient approximations following the VASP code,^{12,13} and the supercells with 18 atoms constructed for both in-phase and anti-phase bondings are presented in Fig. 2. A surface Ga-Ga dimmer bond length of 2.80 Å was

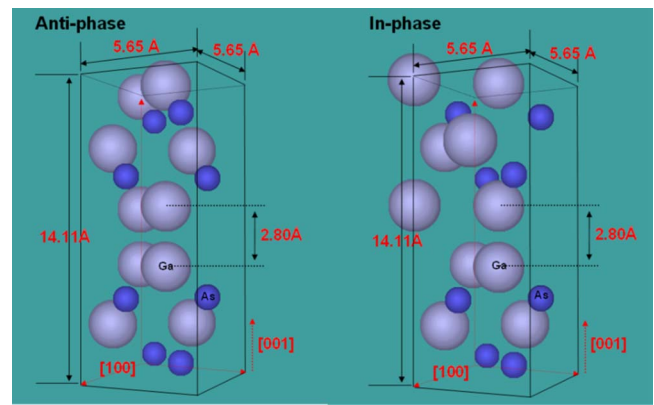


FIG. 2. (Color online) Supercells of anti-phase and in-phase bondings.

adopted.¹⁴ The free energy per cell is -61.4 eV for the anti-phase bonding and -65.2 eV for the in-phase bonding. The energy difference is attributed to the different way of bonding or interface energy variance. This difference can be reduced to be about 2.2 eV after relaxation. Therefore, the interfacial energy of anti-phase bonding is higher than that of in-phase bonding. The higher interface energy tends to stabilize the interfacial oxide layer.¹⁵ Thus, a higher activation barrier of diffusivity for the oxygen in the thin interfacial oxide layer is expected in the anti-phase bonding. These results are also fully supported by a series of studies of transmission electron microscopy analysis which will be presented in another work. Therefore, it is expected that the electrical conductivity is higher for the in-phase bonding as compared to that of anti-phase bonding of *N*-type wafers at 700 °C. However, the trend of conductivity behaves to the contrary that the value associated with anti-phase bonding is much better as compared to that of in-phase bonding at 700 °C as shown in Fig. 1(b). In order to explore this anomalous performance of electrical conductivity due to the bonding phase, high resolution transmission electron microscopy (HRTEM), autocorrelation function (ACF) analysis and energy dispersive x-ray spectroscopy (EDS) point scan are employed to examine the interfacial microstructure in detail.

The ACF method is a statistical analysis of the scanned HRTEM images in real space. The ACF function is equivalent to a two-dimensional form of the Patterson function,¹⁶ well known in x-ray crystallography.¹⁷ And the periodicity of the Patterson function is the lattice constant.¹⁷ Therefore, it is convenient to examine the microstructure of local regions along bonded interfaces with ACF. People have successfully applied the ACF analysis to determine the formation of embedded nanocrystalline silicides in the amorphous interlayer

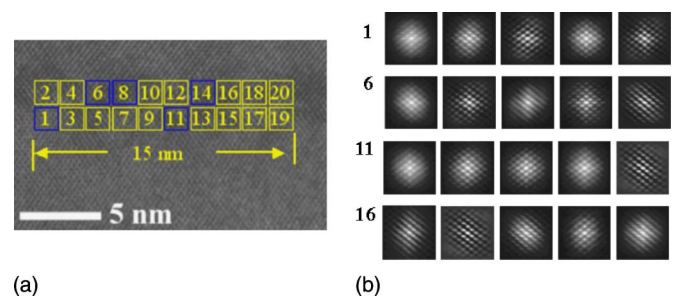


FIG. 3. (Color online) (a) HRTEM micrographs of bonded interface for in-phase *n*-type wafers treated at 700 °C. (b) ACF-processed images of the outlined regions shown in (a).

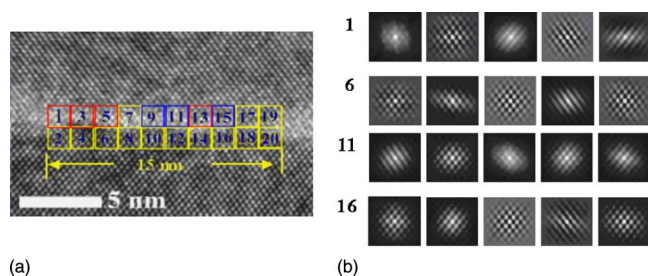


FIG. 4. (Color online) (a) HRTEM micrographs of bonded interface for anti-phase *n*-type wafers treated at 700 °C. (b) ACF-processed images of the outlined regions shown in (a).

of the metal/Si systems.¹⁸ The results of HRTEM and ACF for both in-phase and anti-phase bondings at 700 °C are presented in Figs. 3 and 4, respectively. It is apparent that more nanoscaled disordered phase exists along the interface for the anti-phase bonding by examining the symmetry of ACF functions. Some of the ACF patterns for the anti-phase bonding in Fig. 4(b) preserve less characteristics of crystal symmetry and almost all the ACF plots in Fig. 3(b) for the in-phase bonding preserve such symmetry. This result is anticipated. Due to the higher interfacial energy of the anti-phase interface, the diffusivity of disordered oxides existing in the interface is smaller in the anti-phase bonded wafers than that in the in-phase bonded wafers after thermal annealing. Therefore, the amount of oxides remaining along the bonded interface is higher for the anti-phase bonding than that for the in-phase bonding. Similar ACF results were obtained at other lower temperatures for both *n*- and *p*-type wafers. The chemical analysis from EDS also confirms above argument that more oxygen was detected along the interface for the anti-phase bonding. Also, the existence of nanoscaled oxide in the bonded interface seems to stabilize As atoms and almost equal atomic ratio of Ga and As associated with this oxide was detected. This discovery is consistent with the analysis of GaAs substrate roughening during the oxide desorption.¹⁹

Interfacial defects were found to consist essentially of voids and inclusions, caused by natural topographical irregularities, surface contamination (including native oxide), and solvent residues or trapped gases between the wafers. The causes of bulk and surface defects are more complicated and it is well known from extensive literature in the field that these include dislocations, impurities, vacancies, interstitials, precipitates, and antisite defects.⁸ Arsenic antisite defects (arsenic on gallium sites As_{Ga}) and clusters of other defects are generally known as EL2 (a deep donor in GaAs);²⁰ the concentration of these defects rises with arsenic concentration in the crystal.²¹ When wafers were bonded at elevated temperatures, the evaporation rate of arsenic from the surface was found to be higher than that of gallium (about 2.5 times at 827 °C),²² decreasing the arsenic (and thus the EL2) concentration. A similar phenomenon also can occur at the bonded interface. In a semi-insulating wafer the evaporation of arsenic converts the interface from semi-insulating to *p* type.

This reduction in EL2 (donor) concentration was a major factor responsible for the alteration in electrical resistance in *n*-type GaAs single wafers at a high temperature, but not in the *p*-type wafers.^{6,9} The EDS results clearly show the large deficiency of As atom along the bonded interface at 850 °C. Spreading resistance profiling further provides direct evidence of increased resistance from bonded interface of *n*-type GaAs wafers.

In summary, a continuous interfacial oxide of amorphous Ga_2O_3 at lower temperatures behaves as a current barrier to deteriorate the electrical property. At 700 °C, interfacial oxides shrink and bonded area increases.⁸ The remaining nanoscaled oxides along the interface help to suppress the evaporation of As, which results in the anomalous performance of electrical conductivity, for the anti-phase bonding at 700 °C. At highest treated temperature, 850 °C, of this work, the evaporation of As is severe and the worst electrical performance was observed.

This research was supported by the National Science Council (NSC) of the Republic of China.

¹Q.-Y. Tong, Q. Gan, G. Hudson, G. Fountain, and P. Enquist, *Appl. Phys. Lett.* **84**, 732 (2004).

²F. A. Kish, D. A. Vanderwater, M. J. Peanasky, M. L. Ludowise, S. G. Hummel, and S. J. Rosner, *Appl. Phys. Lett.* **67**, 2060 (1995).

³Z. L. Liau and D. E. Mull, *Appl. Phys. Lett.* **56**, 737 (1990).

⁴T. Akatsu, A. Plöbbs, H. Stenzel, and U. Gösele, *J. Appl. Phys.* **86**, 7146 (1999).

⁵Y. S. Wu, P. C. Liu, R. S. Feigelson, and R. K. Route, *J. Appl. Phys.* **91**, 1973 (2002).

⁶Y. S. Wu, R. S. Feigelson, R. K. Route, D. Zheng, L. A. Gordon, M. M. Fejer, and R. Byer, *J. Electrochem. Soc.* **145**, 366 (1998).

⁷F. Shi, S. MacLaren, C. Xu, K. Y. Cheng, and K. C. Hsieh, *J. Appl. Phys.* **93**, 5750 (2003).

⁸P. C. Liu, C. L. Lu, Y. C. Sermon Wu, J.-H. Cheng, and H. Ouyang, *Appl. Phys. Lett.* **85**, 4831 (2004).

⁹*Appl. Phys. Lett.* (submitted).

¹⁰Y. Okuno, K. Uomi, M. Aoki, T. Taniwatari, M. Suzuki, and M. Kondow, *Appl. Phys. Lett.* **66**, 451 (1995).

¹¹J. W. Mayer and S. S. Lau, *Electronic Materials Science: For Integrated Circuits in Si and GaAs* (Macmillan, New York, 1990), p. 32.

¹²G. Kresse and J. Hafner, *Phys. Rev. B* **47**, RC558 (1993).

¹³G. Kresse and J. Furthmüller, *Phys. Rev. B* **54**, 11169 (1996).

¹⁴G. P. Jing and H. E. Ruda, *J. Appl. Phys.* **79**, 3758 (1996).

¹⁵K. Y. Ahn, R. Stengl, T. Y. Tan, and U. Gösele, *J. Appl. Phys.* **65**, 561 (1989).

¹⁶G. Y. Fan and J. M. Cowley, *Ultramicroscopy* **17**, 345 (1985).

¹⁷B. Fultz and J. M. Howe, *Transmission Electron Microscopy and Diffraction of Materials*, 2nd ed. (Springer, Berlin, 2002), pp. 465–470.

¹⁸S. M. Chang, H. Y. Huang, H. Y. Yang, and L. J. Chen, *Appl. Phys. Lett.* **74**, 224 (1999).

¹⁹T. Van Buuren, M. K. Weilmeyer, I. Athwal, K. M. Colbow, J. A. Mackenzie, P. C. Wong, and K. A. R. Mitchell, *Appl. Phys. Lett.* **59**, 464 (1991).

²⁰O. Oda, D. E. Holmes, H. Yamamoto, M. Seiwa, G. Kano, T. Inoue, M. Mori, H. Shinakura, and M. Oyake, *Semicond. Sci. Technol.* **7**, A215 (1992).

²¹D. E. Holmes, R. T. Chen, K. R. Elliot, C. G. Kirkparick, and P. H. Wu, *IEEE Trans. Electron Devices* **ED-29**, 1045 (1982).

²²C. T. Foxtton, J. A. Harvey, and B. A. Joyce, *J. Phys. Chem. Solids* **34**, 1693 (1973).